

## An Adaptive Neuro-Fuzzy Model to Multilevel Inverter for Grid Connected Photovoltaic System\*

P. Karuppusamy<sup>†</sup> and A. M. Natarajan<sup>‡</sup>

*Bannari Amman Institute of Technology,  
Sathyamangalam, Erode (DT), Tamilnadu 638401, India*

<sup>†</sup>*eee\_k1983@yahoo.co.in*

<sup>‡</sup>*amn@bannari.co.in*

K. N. Vijeyakumar

*Dr. Mahalingam College of Engineering and Technology,  
Pollachi, Tamilnadu, India*

*vijey.tn@gmail.com*

Received 18 June 2014

Accepted 31 December 2014

Published 13 February 2015

This paper proposed an adaptive neuro-fuzzy model (ANFIS) to multilevel inverter (MLI) for grid connected photovoltaic (PV) system. The purpose of the proposed controller is that it is not requiring any optimal pulse width modulated (PWM) switching-angle generator and proportional–integral controller. The proposed method strictly prohibits the variations present in the output voltage of the cascaded H-bridge MLI. In this method, the ANFIS have the input which is grid voltage, the difference voltage and the output target is control voltage. By using these parameters, the ANFIS makes the rules and has been tuned perfectly. During the testing time, the ANFIS gives the control voltage according to the different inputs. The resultant control voltage equivalent gate pulses are utilized for controlling the insulated gate bi-polar switches (IGBT) of MLI. Then the ANFIS based MLI for grid connected PV system is implemented in the MATLAB/simulink platform and the effectiveness of the proposed control technique is analyzed by comparing with the neural network (NN), fuzzy logic control, etc. The comparison results demonstrate the superiority of the proposed approach and confirm its potential to solve the problem. A prototype of three-phase grid connected cascaded H-bridge inverter has been developed using field-programmable gate array (FPGA) and results are analyzed.

*Keywords:* PV; cascaded multilevel inverter; grid voltage; control voltage; ANFIS; FPGA.

### 1. Introduction

In last decade in most of the countries, the environmental crisis and their economical evolutions are enforced into deep exploration in renewable energy. The most

\*This paper was recommended by Regional Editor Piero Malcovati.

<sup>†</sup>Corresponding author.

scrutinize technologies are Hydro, photovoltaic (PV) and wind energy conversion. Among these technologies, PV system is most standard and environmentally affable technology.<sup>1</sup> Photovoltaic system advantages are efficiency, authenticity, easily implementation, economic in cost and lesser in environmental effect and also ability to carry micro grid systems, and to connect to the electric grid.<sup>2,3</sup> It is the most substitute system for those who emanate electricity and is also used for remote applications.<sup>4,5</sup>

Solar energy is converted into electrical energy by using PV arrays.<sup>6</sup> The merits of PV arrays are spotless, inexhaustible and economic in cost and also lesser in maintenance. For these conversions, PV systems needed power converters, placed between PV arrays and the grid,<sup>7</sup> because PV arrays are performed at maximum power point tracking (MPPT)<sup>8,9</sup> and to infuse alternating current into the grid. There are two types of power connectors.<sup>10,11</sup> (i) DC/DC power converter. (ii) DC/AC power converter. DC/DC power converter is used to perform the PV arrays at the peak power point. DC/AC power converter is used to join the PV system to the grid.<sup>12</sup> The few advantages of these two converters are less distortion, shrinking switching frequency, diminishing dv/dt stress and so on.<sup>13,14</sup> By this technique, few multilevel topologies exercised to PV systems.<sup>15</sup>

The three fundamental characteristics of multilevel inverter (MLI) topologies are neutral-point-clamped and flying-capacitor MLIs and cascaded H-bridge MLI (CHB-MLI). In these MLI topologies, flying-capacitor MLIs needs single DC source, which is a major disadvantage. But it becomes popular in case of photo voltaic systems. Because solar cells needs individual generators for gathered.<sup>16</sup> According to that, CHB-MLI is having more features than others also having extra advantages are no need for DC/DC booster, decline in power drops due to sun darkening, consequently, efficiency will increase therefore more reliability.<sup>19</sup> But the significant obstacle in multilevel converter is complication in control and their pulse width modulator.<sup>17,18</sup> Also implementation of conventional space-vector pulse width modulated (PWM) current regulator is difficult.<sup>20</sup>

This paper projected an adaptive neuro-fuzzy model (ANFIS) to MLI for grid connected PV system. The intention of the proposed controller is not requiring any optimal PWM switching-angle generator and proportional–integral controller. In this technique, it hinders the fluctuation in the output voltage of the cascaded H-bridge MLI. The input voltages are grid voltage, difference voltage and the output voltage is control voltage. According to this, ANFIS can be in control and tuned accurately. According to various inputs, the ANFIS generates the control voltage at a time of testing. The output voltage equivalent gate pulses are used for handling the insulated gate bi-polar switches (IGBT) of MLI. The remaining of the paper is coordinated as follows: the recent research works is evaluated in Sec. 2; the proposed work brief explanation is elucidated in Sec. 3; the proposed controlling technique is described in Sec. 4; Simulation results and the similar discussions are given in Sec. 5; Experimental results and discussions are given in Sec. 6; and Sec. 7 ends the paper.

## 2. Recent Research Works: A Brief Review

In this paper, so many applications are accessible which depends on MLI with PV applications. Few of them are analyzed. Carlo Cecati *et al.*<sup>21</sup> have examined converter for PV systems includes two stages: A DC/DC booster and a PWM inverter. They project a single-phase H-bridge multilevel converter for PV systems controlled by an integrated fuzzy logic controller (FLC)/modulator. The uniqueness of the projected system are utilizes of a fully FLC and utilizes of an H-bridge power-sharing algorithm. The essential signal processing was auctioned by a resulting in a fully integrated system-on-chip controller, mixed-mode field-programmable gate array (FPGA). The common architecture of the system and its execution in a extreme manner were obtainable and examined.

Seyezhai *et al.*<sup>22</sup> have proposed a MLI. This is an advanced topology high voltage DC–AC conversion. For fuel cell function silicon carbide (SiC) switches are used in a hybrid MLI, and they also aim on a double orientation modulation technique. Stair the carrier waveform, and the projected waveform performs two reference waveforms and a solitary inverted sine wave. While in the output voltage spectral quality and switching losses was contrast with the conventional dual carrier waveform. The execution of the inverter obtained from the theory and simulation has been explored.

Chandralekha *et al.*<sup>23</sup> have presented the escalation in a wind turbine driven induction generator subsystem, joint power system with solar cell subsystem, and diesel generator set. Solar cells would produce the power only in day time and also the turbine driven IG varies according to the velocity of wind. Constant power supply is assured by the subsystem exercised in tandem and with battery backup. Peoples in remote areas such as villages in hill tops where power supply may not be present, but the amalgamation afford a constant power supply. For generating a constant voltage and frequency AC power supply for function and business applications, the power electronic scheme projected which engages a choice of power source inverter.

Vijayalakshmi *et al.*<sup>24</sup> have presented regarding to the assignment based on a high conversion ratio hybrid DC–DC converter fed single-phase low harmonic distortion nine-level PV inverter topology for PV power conditioning systems (PCSs) with a PWM control scheme. In microcontroller PIC16C7F88, a digital PI control algorithm is implementing in it. Before making it to AC for grid tie applications to convert the energy sources to a higher-voltage DC, a PCS is necessary for low voltage DC sources. The endeavor of this venture is to begin and confer the main aspects of novel topologies that deal with design problems.

Three-phase cascaded H-bridge converter is architect for a stand-alone PV purposes. It is presented by Raghu Vamsi Goutham *et al.*<sup>25</sup> Several H-bridge cells coupled in series and each one linked to a string of PV modules in the multilevel topology. The adopted control system allows the self-governing control of each DC-link voltage, implementing, in this way, the tracking of the most power point for each

string of PV panels in addition to less ripple sinusoidal-current waveforms are obtained with one power factor. Another advantages like perform at lower switching frequency or lower current ripple contrast to standard two-level topologies. For distinct performing conditions simulation and experimental results were analyzed. A control method for three-phase multilevel cascaded H-bridge inverter for PV system has presented by Valan Rajkumara *et al.*<sup>26</sup> The MPPT has the ability of dig out the peak power from the PV array allied to each DC link voltage level. This algorithm was worked out by perturbation and observation (P&O) method. The alterations of modulation index and phase angles were amalgamated onto FPGA by means of hardware description language (VHDL).

The optimization of switching angle of a adapt H-bridge single-phase seven-level inverter for stand-alone PV system was presented by Krismadinata *et al.*<sup>27</sup> The inverter embraces a conventional H-bridge inverter and two bidirectional switches and it could produce a seven-level output voltage level, namely +Vdc, +2/3Vdc, +1/3Vdc, 0, -1/3Vdc, -2/3Vdc and -Vdc. To enhance the output waveform better, optimized harmonic elimination stepped waveform (OHESW) method was performed. From OHESW, Newton-Raphson method was employed to solve the transcendental equations which creates all feasible elucidations with any random primary presumptions.

The MLI is widely used as the most modular and environmentally friendly technologies which are reviewed from the recent research works. The MLI topology plays an important role for rectifying the switching losses, the voltage stress, the total harmonic distortion (THD) and the high switching frequency in solar power generation system. Different MLI topologies are used in solar power generation (PV). The topology is varied due to the output variation and THD of inverter; also, the topology design is a complex task. By different essential topologies like single phase cascaded H-bridge MLI, diode-clamped MLI and single phase five-level inverter the problems are overcome. For the unknown load and parameter variations, the above existing models depend on the precise topology of the system and the topologies cannot be adaptive. So the effective control technique is needed for the MLI, which is explained in the following Sec. 3.

### 3. Proposed Control Technique Using MLI for PV Applications

In solar power generation system, the MLI topology plays an important role for rectifying the switching losses, the voltage stress, the THD and the high switching frequency. In solar power generation (PV), different MLI topologies are used. Because the MLI has better working performance compared to the conventional PWM inverters. It provides even voltage sharing, both statically and dynamically; reduce the size and volume due to the elimination of the bulky coupling transformers or inductors. But the topology is varied due to the output variation and THD of inverter. The topology design is a complex task since the topologies cannot be adaptive

for the unknown load and parameter variations. So it needs an efficient control structure to overcome the mentioned drawbacks. The required control system is explained in Fig. 1 and the detailed explanation about the control structure is described.

The structure explains the proposed control structure, which contains PV panels connected with the each H-bridge of MLI. The three phase MLI output ( $V_a$ ,  $V_b$  and  $V_c$ ) is given to the grid, i.e., known as grid voltage ( $V_g$ ). The grid voltage variation is determined from the comparator, which evaluates the difference between the PV voltage ( $V_{pv}$ ) and the grid voltage ( $V_g$ ). In the difference, voltage ( $V_d$ ) and the grid

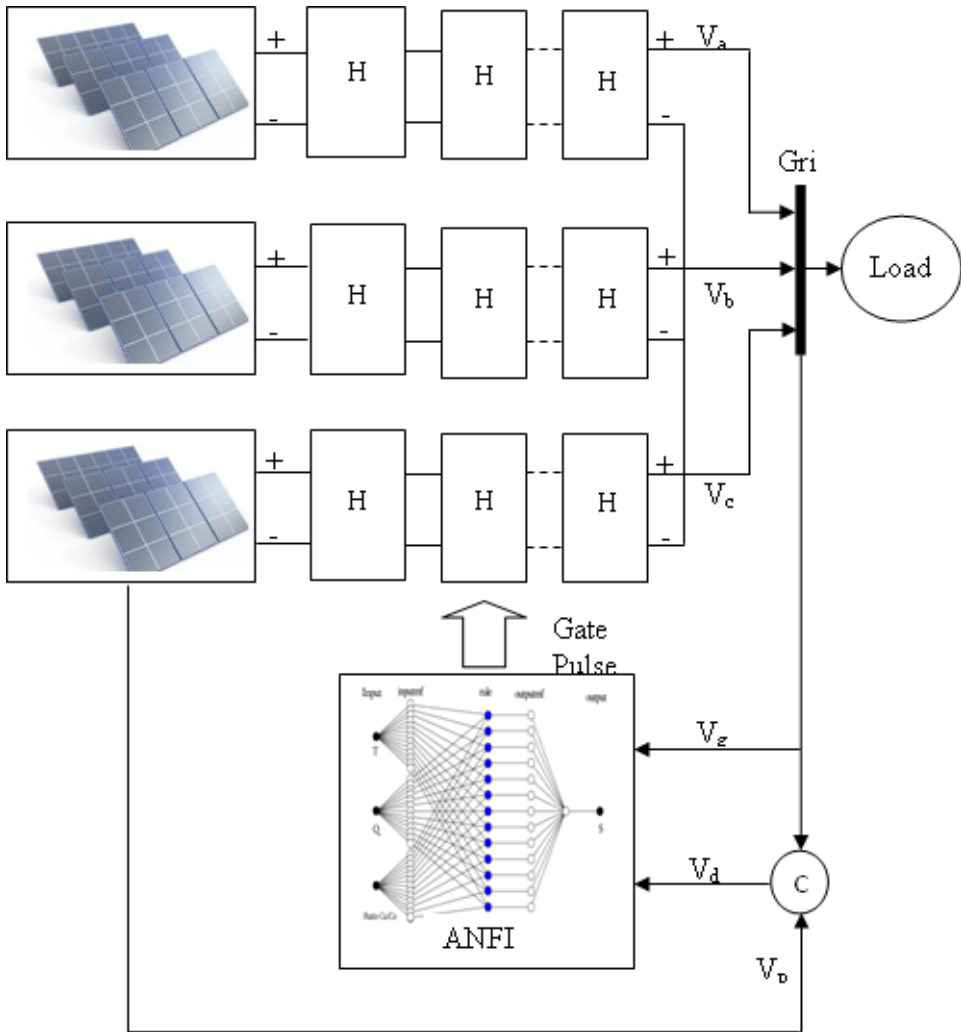


Fig. 1. Structure of the proposed control technique.

voltage ( $V_g$ ) are used as the input of the ANFIS. The output of the ANFIS structure is the controlled voltage ( $V_{cn}$ ); it is converted into the corresponding gate pulses to operate the MLI. The detailed explanations about the presented PV panel, MLI for PV applications are given in the following section.

### 3.1. PV panels

The PV cell is an electrical device, which is used to convert the light energy into electricity. The solar PV energy is known by sustainable energy. When the sunlight photons strike the surface panel and are absorbed by the semiconductor, i.e., silicon. The electrons are knocked loose from their atoms, which makes an electric potential difference. Resultant current starts flowing through the material to cancel the potential and this electricity is captured. The PV cell current flow is described in the following Eq. (1)

$$I_{pv} = \frac{I_{mp}}{1 - C^{-d}} \left[ e^{\frac{V_{oc}}{a}} + \frac{q(V+R_s I)}{mkT} - e^{\frac{V_{oc}}{a}} \right] - \frac{V + R_s I}{R_{sh}}, \quad (1)$$

where  $q$  is the electron charge ( $1.6 \times 10^{-19} C$ ),  $k$  is Boltzmann's constant ( $1.38 \times 10^{-23} J/K$ ),  $T$  is the temperature in  $K$  and  $N_s$  is the number of cells of the module,  $V_{oc}$  is the open circuit voltage,  $I_{mp}$  is the current at maximum power,  $m$  is the cell recombination coefficient ( $1 < m < 3$ ),  $I$  is the current and  $R_s$  is the series resistance. The MLI is explained in Sec. 3.2.

### 3.2. MLI for PV applications

The  $n$  number of bridges connected with the  $h$  number of DC generators like PV cells, which is known by a single phase topology. Three phase topology can be realized by star or delta connection of three single phase topologies. Generally the H-bridge consists of four IGBT and one DC source. The number of output phase voltage levels of cascade MLI is  $2h + 1$ , where  $h$  is the number of DC generators. The output phase voltage of the  $n$ -level inverter is  $n$ -level staircase waveform. The fundamental output voltage of the MLI can be described in the following Eq. (2).

$$V(t) = \sum_{n=1}^{\infty} (a_n \sin n\alpha_n + b_n \cos n\alpha_n), \quad (2)$$

where  $V(t)$  is the output voltage,  $a_n$  is the odd harmonics,  $b_n$  is the even harmonics, which is zero because of the quarter wave symmetry of the output voltage,  $\alpha$  is the switching angle. The odd harmonics at  $n$  order is described in the following Eq. (3)

$$a_n = \frac{4}{n\pi} \sum_{s=1}^{\infty} V_{dc}^n [\cos(n\alpha_1) + \cos(n\alpha_2) + \dots + \cos(n\alpha_s)] \sin(n\omega t) \quad (3)$$

$0 < \alpha_1 < \alpha_2 \cdots \alpha_k < \frac{\pi}{2}$  and

$$\text{THD} = \sqrt{\frac{\sum_{k=2}^n [V(t)]^2}{V_1}}, \quad (4)$$

where  $V_{dc}$  is the input DC voltage. In this method consider the 7-level inverter; it consists of  $h = 2$  number of bridges. The output phase voltage is the sum of all the individual bridge outputs. The 7-level inverter output voltage variation and THD is identified from the above mentioned equations. The MLI normal and abnormal condition outputs are the required dataset to train the ANFIS. During the testing time, the ANFIS develops the optimum control voltage, which is converted into controlling pulses to control the inverter switches. The detailed explanation about the proposed controlling technique is described in Sec. 4.

#### 4. Control Voltage Generation using ANFIS

ANFIS is an adaptive network which permits the usage of neural network (NN) topology together with fuzzy logic. It not only includes the characteristics of both methods, but also eliminates some disadvantages of their lonely-used case. Operation of ANFIS looks like feed-forward back propagation network. Consequent parameters are calculated forward while premise parameters are calculated backward. There are two learning methods in neural section of the system: Hybrid learning method and back-propagation learning method. In fuzzy section, only zero or first order Sugeno inference system or Tsukamoto inference system can be used. Since ANFIS combines both neural network and fuzzy logic, it is capable of handling complex and nonlinear problems. Even if the targets are not given, ANFIS may reach the optimum result rapidly. ANFIS reaches to the target faster than NN. When a more sophisticated system with a huge data is imagined, the use of ANFIS instead of NN would be more useful to overcome faster the complexity of the problem. In training of the data, ANFIS gives results with the minimum total error compared to other methods.

ANFIS is a hybrid soft computing model, i.e., combination of neuro-fuzzy and NN, which contains high level reasoning capability and low level computational power.<sup>28</sup> The ANFIS constructs a fuzzy interference rules depending on the input and the output target. The fuzzy interference mechanism is tuned by the NN learning mechanism. Generally the ANFIS has a layered structure, which is described in Fig. 3. It consists of five different layers such as input layer, fuzzification layer, product layer, normalization layer and defuzzification layer. The nodes are represented as both adaptive and fixed nodes, i.e., the square nodes are adaptive nodes and the circle nodes are fixed nodes. In this proposed method, the ANFIS inputs are may be the grid voltage  $V_g$  and the difference voltage  $V_d$  and the output target is control voltage  $V_{cv}$ . By using these parameters, the ANFIS has been making the rules and tuned perfectly.

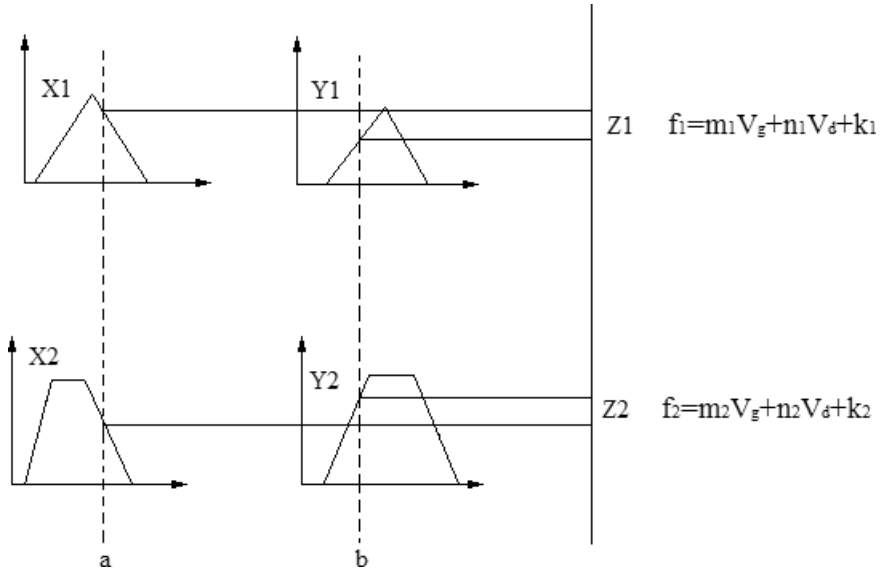


Fig. 2. First-order Takagi–Sugeno fuse reasoning.

The inputs of the ANFIS are the grid voltage ( $V_g$ ) and the difference voltage ( $V_d$ ), which is described in the following. For first order Takagi–Sugeno inference system with two fuzzy a common rule set is described in the following Eqs. (5) and (6)

$$\text{Rule 1 : If } V_g \text{ is } C_1 \text{ and THD is } D_2 \text{ then } f_1 = m_1 V_g + n_1 V_d + k_1, \quad (5)$$

$$\text{Rule 2 : If } V_g \text{ is } C_2 \text{ and THD is } D_2 \text{ then } f_2 = m_2 V_g + n_2 V_d + k_2, \quad (6)$$

where  $m_1, m_2, n_1, n_2, k_1$  and  $k_2$  are the linear parameters,  $C_1, C_2, D_1$  and  $D_2$  are the nonlinear parameters. Figure 2 shows the fuse reasoning of the ANFIS.

Activation levels of the fuzzy rules are calculated using  $W = X_i(a) \bullet Y_i(b)$ , where the logical operator “and” may be modeled by a continuous  $t$ -norm, and in this case, it is expressed as a product. The individual output of each rule is obtained as a linear combination between parameters of the antecedents of each rule as given in the following Eq. (7).<sup>29</sup>

$$f_i = m_i V_g + n_i V_d + k_i, \quad i = 1, 2, \dots \quad (7)$$

The output of the model  $f$  is obtained by multiplying the standardized activation degrees of the rules by the individual output of each rule, which is expressed in the following Eq. (8)

$$f = \frac{\sum \bar{W}_i f_i}{\sum W_i}, \quad i = 1, 2, \dots \quad (8)$$

where  $W_i$  is the normalized value, which is the sum of  $W_1$  and  $W_2$ . The ANFIS layer structure is described in Fig. 3 and the corresponding description is given below.

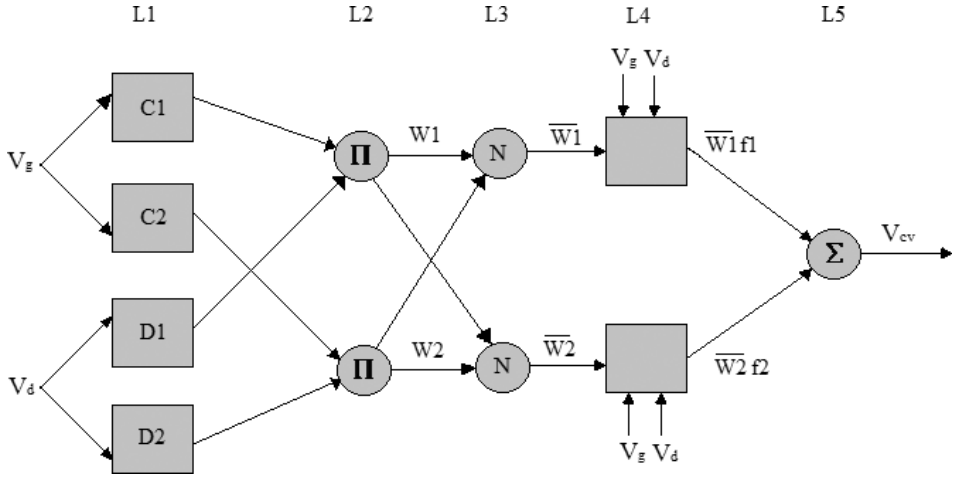


Fig. 3. Structure of the ANFIS.

#### 4.1. Fuzzification layer

In this mode, each input layer represents an input variable and it is transmitted into fuzzification layer. The grid voltage ( $V_g$ ) and the difference voltage ( $V_d$ ) of nodes are  $C_1, C_2, D_1$  and  $D_2$ , in which  $C_1, C_2, D_1$  and  $D_2$  are linguistic labels of fuzzy theory for dividing the membership functions.

The output of the fuzzy layer is given in the following Eqs. (9) and (10)

$$R_{L1,i} = \mu C_i(V_g), \quad i = 1, 2, \tag{9}$$

$$R_{L1,j} = \mu D_j(V_d), \quad j = 1, 2, \tag{10}$$

where  $R_{L1,i}$  and  $R_{L1,j}$  are the output of the fuzzy layer and  $\mu C_i(V_g)$  and  $\mu D_j(V_d)$  are the membership function of the fuzzy layer.

#### 4.2. Product layer

This layer performs logical “and” or product of the input membership functions, which is labeled as  $\pi$ . The product layer output is the input weight function of the next node. The output of this layer can be described by the following Eqs. (11) and (12)

$$W_1 = R_{L2,i} = \mu C_i(V_g) \cdot \mu D_i(V_d), \quad i = 1, 2, \tag{11}$$

$$W_2 = R_{L2,j} = \mu C_j(V_g) \cdot \mu D_j(V_d), \quad j = 1, 2, \tag{12}$$

where  $W_1$  and  $W_2$  are the outputs of the product layer.

### 4.3. Normalization layer

The normalized layer is the third layer, in which each node is a fixed one that represents the IF part of a fuzzy rule. It is used to normalize the input weights, which can perform the fuzzy “and” operation. This layer may label as N and the output of this layer is given in the following Eqs. (13) and (14)

$$\bar{W}_1 = R_{L3,i} = \frac{W_i}{W_1 + W_2}, \quad i = 1, 2, \quad (13)$$

$$\bar{W}_2 = R_{L3,j} = \frac{W_j}{W_1 + W_2}, \quad j = 1, 2, \quad (14)$$

where  $\bar{W}_1$  and  $\bar{W}_2$  are the outputs of the normalized layer.

### 4.4. Defuzzification layer

This layer performs an adaptive function, which gives output membership function based on predetermined fuzzy rules. The output of this layer is given in Eqs. (15) and (16)

$$\bar{W}_1 f_i = R_{L4,i} = \frac{W_i}{W_1 + W_2} [m_1 V_g + n_1 V_d + k_1], \quad (15)$$

$$\bar{W}_2 f_j = R_{L4,j} = \frac{W_j}{W_1 + W_2} [m_2 V_g + n_2 V_d + k_2], \quad (16)$$

where  $\bar{Z}_1 f_i$  and  $\bar{Z}_2 f_j$  are the outputs of the defuzzy layer.

### 4.5. Total output layer

The output layer represents the THEN part of the fuzzy rule. The total of the input signals can be calculated, which is labeled as  $\Sigma$ . The total output of the layer is given in the following Eq. (17)

$$f = R_{L5,i} = \sum \bar{W}_l f_i = \frac{\sum \bar{W}_i f_i}{\sum W_i}, \quad (17)$$

where  $f$  is the total output, once the ANFIS training is finished, it is ready to give the control voltage ( $V_{cn}$ ) to reduce the output variation and THD of the MLI. Once the process is over, the ANFIS is ready to give the control voltage for the various input grid voltage and difference voltage. Then the proposed control technique is implemented in the MATLAB/simulink platform and the effectiveness is tested by the comparison with other techniques. The brief description about the proposed method implementation and the corresponding discussion is given in the following Sec. 5.

## 5. Simulation Results and Discussions

The proposed method is implemented in MATLAB/simulink 7.10.0 (R2012a) platform, 4GB RAM and Intel(R) core(TM) i5. The MLI output voltage and current of the three phases, filter voltage; the output voltage before and after filter was analyzed. Also with that in this method the effect of RL and RC load in the inverter current in each phase and the variation of active and reactive power, inverter voltage and current requested by the load and the voltage sag were analyzed. By the analysis of the THD of the voltage and current with normal, neural, fuzzy and ANFIS method, it was proved that the proposed method is more effective when compared with the previous method. The analysis of the results is discussed in the following.

The MLI normal output voltage of the a-phases was represented in Fig. 4. Similarly, the MLI phase current for normal time is explained in Fig. 5. These results show that the required 7-level inverter is working without any fault.

The variations of output voltage before and after filter in phase is shown in Fig. 6. But in both before and after filter, the voltage magnitude get reduced during the same time period (i.e., 0.1–0.2s) when the DC voltage gets reduced. The proposed system shows better performance in the output voltage even there is a variation in the input DC voltage. Different loads were considered in order to evaluate the performance of the ANFIS in particular, the series RC and RL loads were considered. Figures 7 and 8 shows that, whatever the load (leading or lagging), the output

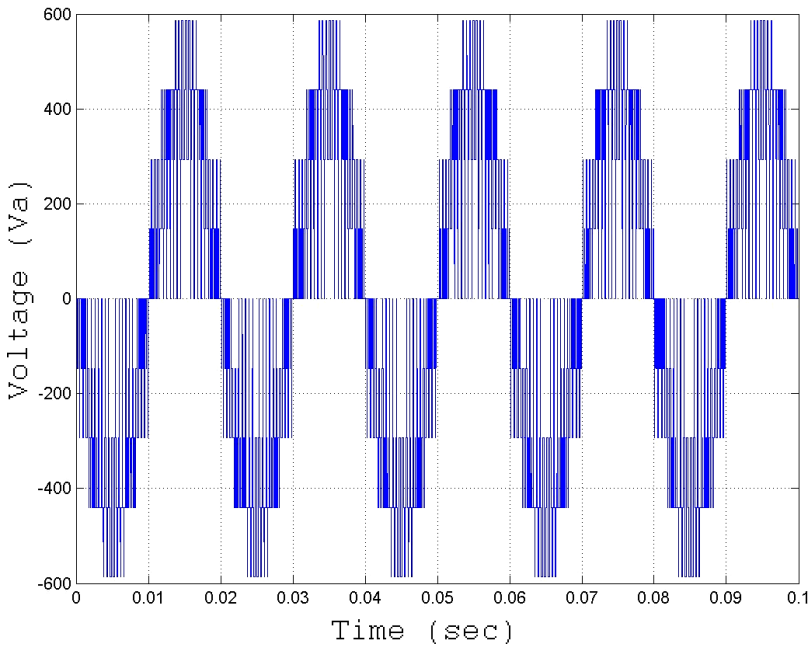


Fig. 4. MLI output voltage of a-phase.

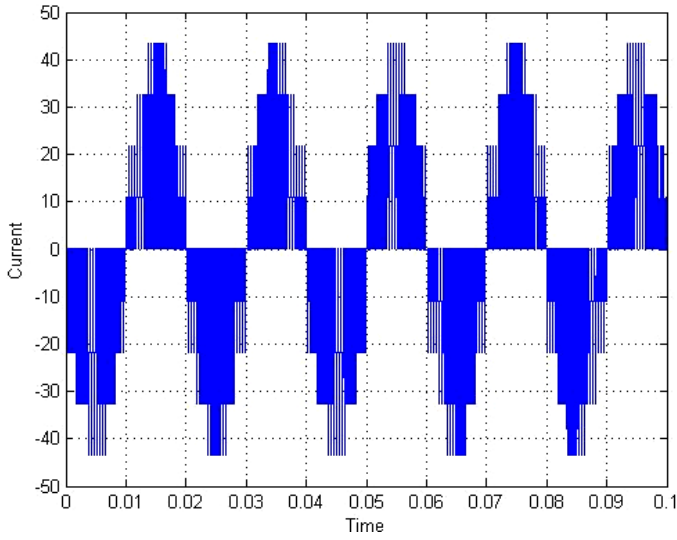


Fig. 5. MLI output current of a-phase.

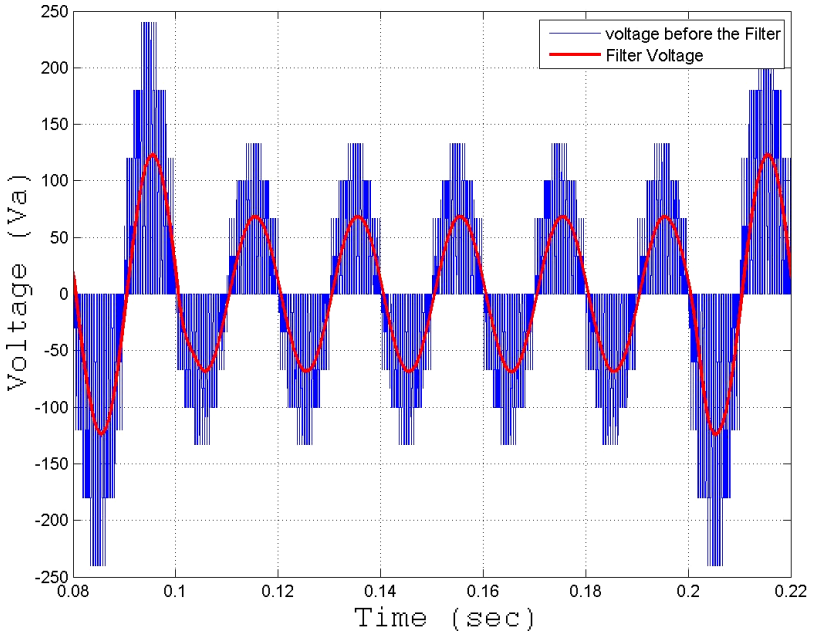


Fig. 6. Output voltage before and after filter.

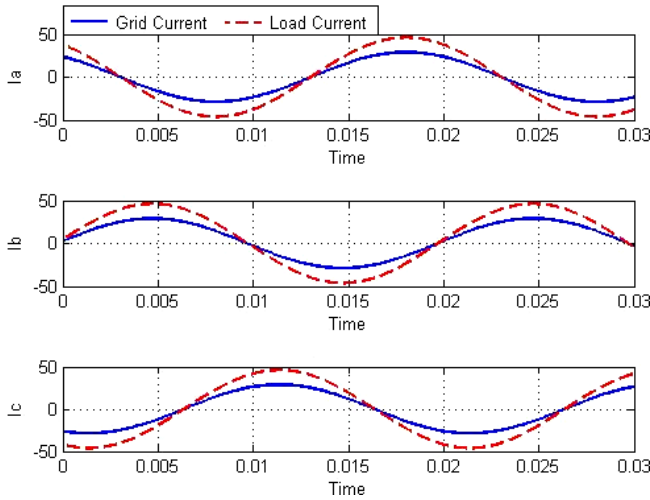


Fig. 7. MLI with RC load.

current follows its reference. It can be noticed that the inverter current was synchronized with the grid voltage. Figure 9 shows the grid current and load current results for varying the active and reactive power requested by the load.

Results shown in Figs. 10 and 11 revealed the THD analysis of the inverter voltage and current in the proposed method (i.e., ANFIS). The voltage and current

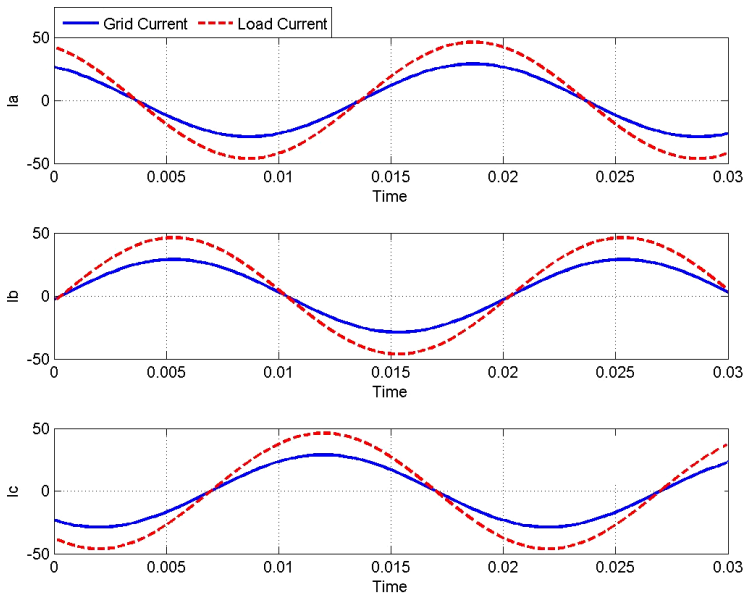


Fig. 8. MLI with RL load.

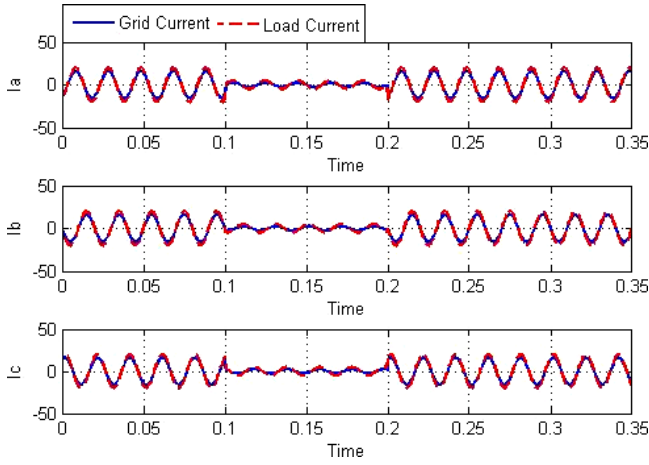


Fig. 9. Variation of the active and reactive power requested by the load.

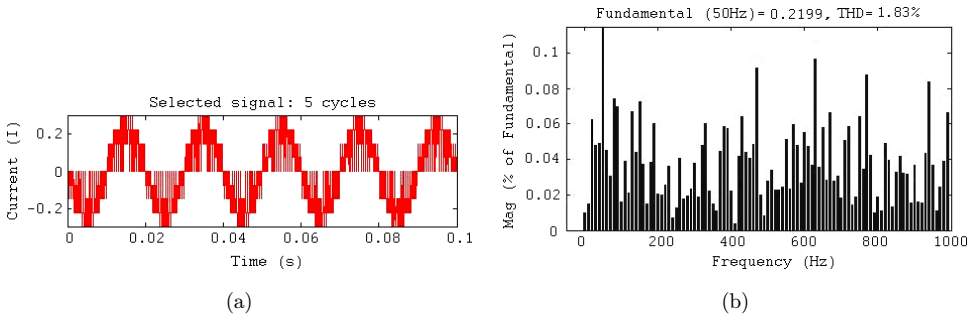


Fig. 10. THD analysis of output current with ANFIS method: (a) selected 5 cycles of voltage, (b) THD.

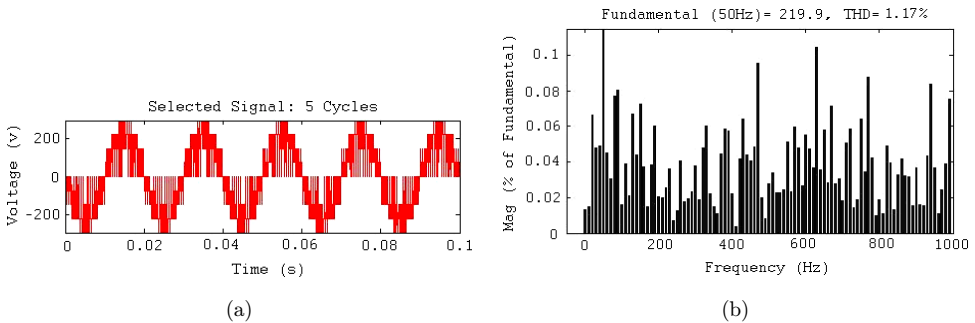


Fig. 11. THD analysis of output voltage with ANFIS method: (a) selected 5 cycles of voltage, (b) THD.

Table 1. THD comparison for simulation.

Percentage THD of the MLI				
Method	Normal <sup>30</sup>	NN <sup>32</sup>	Fuzzy <sup>33</sup>	ANFIS
Voltage THD	2.7%	5.29%	1.48%	1.17%

Table 2. Efficiency comparison.

Efficiency			
Normal	NN	Fuzzy	ANFIS
90.9%	91.6%	92.3%	93.7%

percentage of THDs of the MLI in different methods were tabulated in Table 1. The effectiveness of the harmonic elimination process has been determined by the THD analysis of the MLI among without controller, NN, fuzzy and proposed ANFIS. During the THD analysis process, 5 cycles of MLI voltage has been selected for every control technique. From the THD analysis, amount of THD present in the MLI output voltage without controller is 2.7%. Proposed method, the high THD affect the MLI output voltage presented with distortions and this reduced the power quality. By using the NN control technique in the MLI, which contains the THD in the output voltage is 5.29% and by using the fuzzy control technique, the THD in the output voltage is 1.48 %. The amount of THD present in the output voltage is much reduced by using the proposed ANFIS controller. THD presents in the MLI output voltage with ANFIS controller is 1.17%. Similarly the proposed method efficiency is compared with the above mentioned techniques, which is shown in Table 2. In this paper, the MLI output and the corresponding efficiency for normal method, NN technique, fuzzy and proposed method is analyzed. The comparison results prove the effectiveness of the proposed control technique. The brief description about hardware implementation and the corresponding discussion is given in Sec. 6.

## 6. Experimental Results

A prototype of three-phase grid connected cascaded 5-level inverter has been developed using above described scheme and tested in the laboratory. Experimental results have been chosen to show the effectiveness of the proposed configuration. The voltage of grid is 220 V, 50 Hz. IRF250 MOSFETs are chosen for the power devices with rating of 30 A, 200 V, 0.085 Ohm, N-Channel Power MOSFET. The Spartan-3E family of FPGAs is used to implements the PWM signal generation, the current controller, and the proposed modulation. The FPGA is specifically designed to meet the needs of high volume, cost-sensitive consumer electronic applications.

The MLI output voltage and current of the three phases: The grid voltage and current was analyzed. Also with that, in this method, the analysis of the THD of the voltage and current were analyzed. The analysis of the results is discussed in the following paper. Output results are obtained by using Yokogawa's WT 1800 power analyzer.

The grid voltage and the 3-phase MLI output voltage was represented in Fig. 12. Similarly, the grid current and 3-phase MLI current was represented in Fig. 13.

Figure 12 shows the 3-phase grid voltage (U1, U2 and U3) with the inverter voltage of 220 V (U4, U5 and U6). Similarly, Fig. 13 shows the 3-phase grid current, (I1, I2 and I3) with the inverter current of 0.98 A (I4, I5 and I6). The synchronized waveform of B phase grid voltage (U2) and inverter B phase voltage (U5) are shown in Fig. 14. The 5-level MLI R phase voltage and R phase current is shown in Fig. 15. The synchronized grid current and inverter current is shown in Fig. 16.

The efficiency and THD measurements were performed using an Yokogawa's WT 1800 power analyzer. Advantages of power analyzer are high-precision, wide range, fast-sampling, simultaneous harmonic measurement.

The 5-level MLI output voltage THD and current THD charts are shown in Figs. 17 and 18 respectively. The THD of the output voltage is 1.32% and current

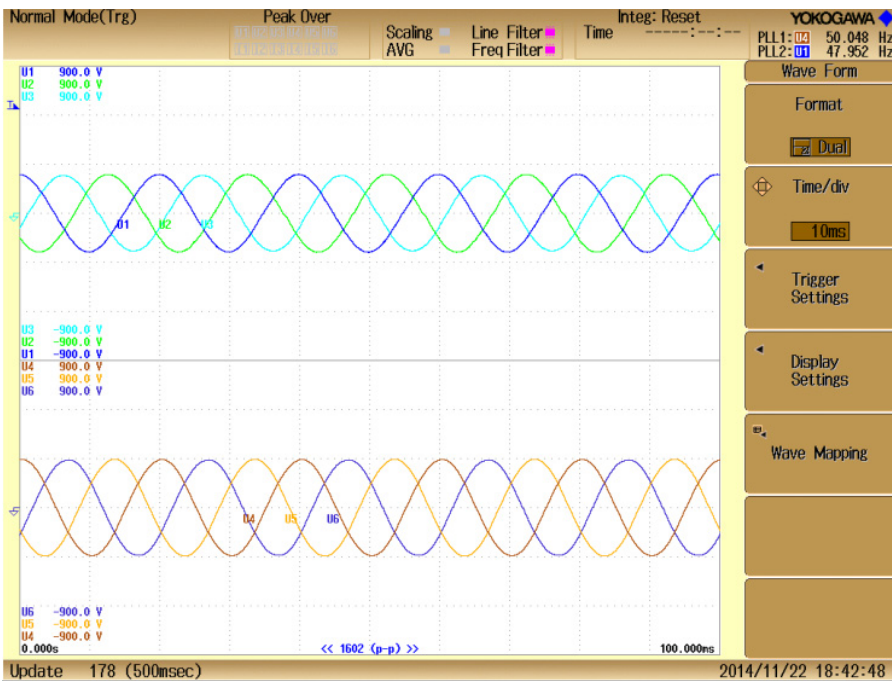


Fig. 12. Experimental result of grid voltage with 3-phase MLI output voltage. Time base 10 ns/div.



Fig. 13. Experimental result of grid current with 3-phase MLI Current. Time base 10 ns/div.

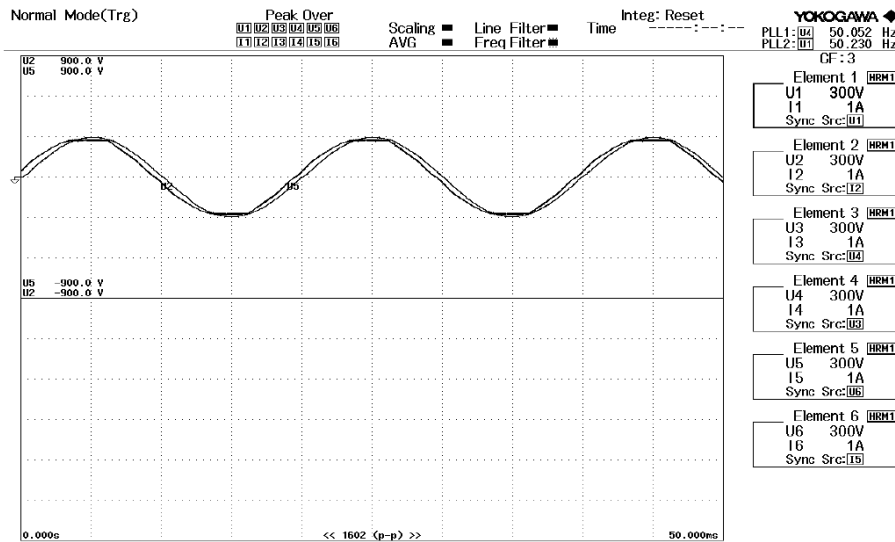


Fig. 14. Experimental result of grid R phase voltage the inverter R phase voltage. Time base 5 ns/div.



Fig. 15. Experimental result of MLI 5-level output voltage. Time base 5 ns/div.

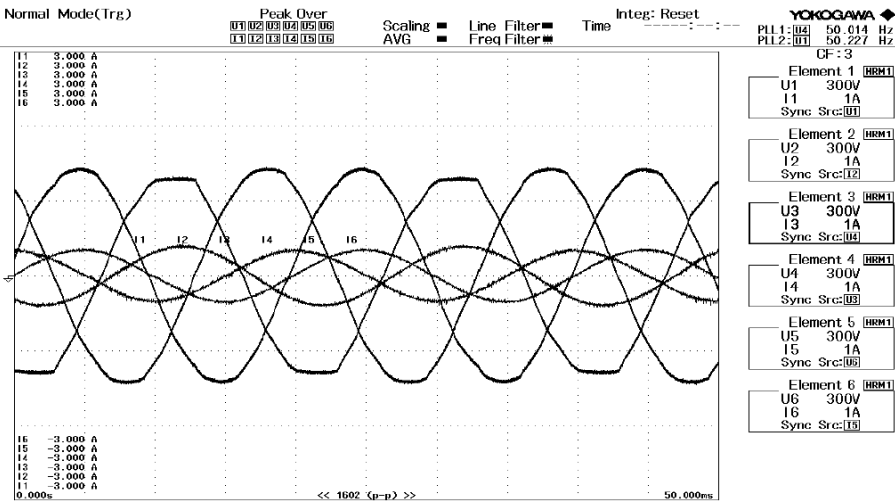


Fig. 16. Experimental result of grid current with inverter current. Time base 5 ns/div.

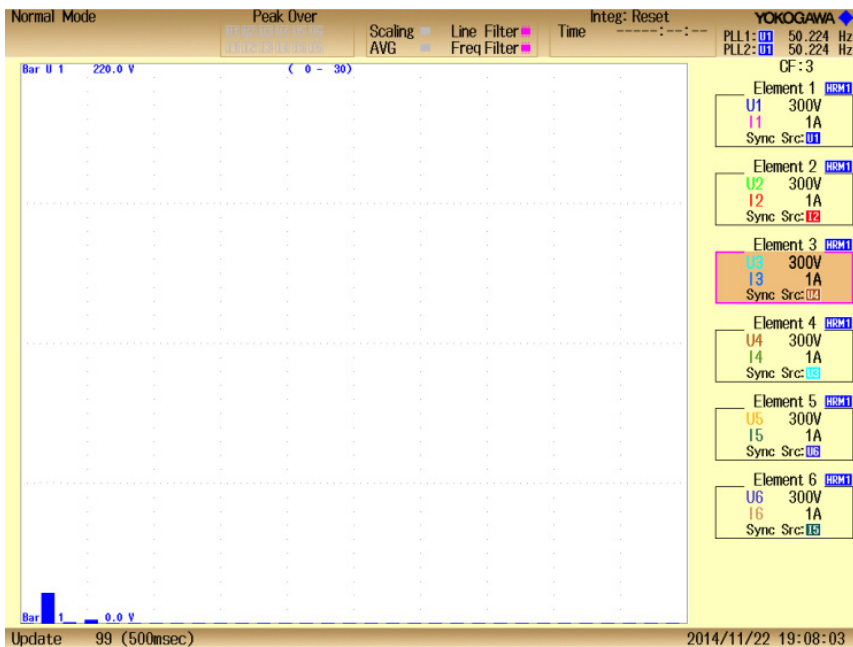


Fig. 17. Voltage THD of the MLI Y-axis 7.5%/div.

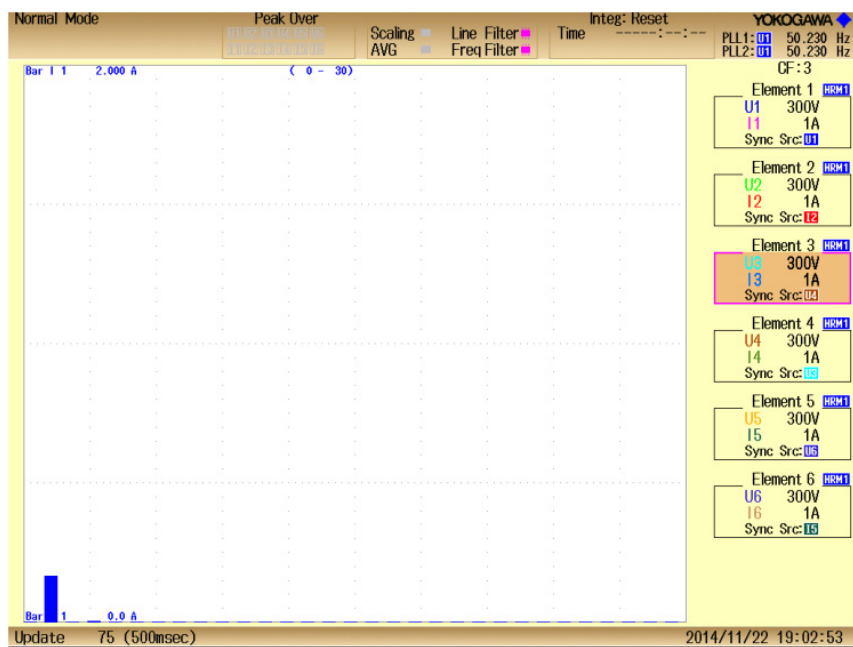


Fig. 18. Current THD of the MLI Y-axis 7.5%/div.

Table 3. THD comparison for experimental results.

Method	THD of the MLI			
	Normal (1) <sup>30</sup>	NN <sup>32</sup>	Fuzzy <sup>33</sup>	Proposed method
Voltage THD	4.19%	8.7%	15.6%	1.32%

THD is 1.89%. The experimental voltage and current percentage of THDs of the MLI in different methods were tabulated in Table 3.

The THD percentage for simulation and experimental are verified through the research work.<sup>30,31</sup> In the research work,<sup>30</sup> a 9-level MLI is used to connect with grid using transformer less PV Systems, which has simulation voltage THD of 2.7% and experimental voltage THD of 4.19%. In the research work,<sup>31</sup> Modular MLI with new modulation method is used for PV grid connected generator, which has simulation voltage THD of 3.6% and experimental voltage THD of 4.2%. The comparison results prove the effectiveness of the proposed control technique.

## 7. Conclusion

This paper proposed an ANFIS to MLI for grid connected PV system and it is simulated in the MATLAB platform. With the enhanced knowledge rules based on the proposed ANFIS generate switching angles for the appropriate voltage variations, the proposed method performances were compared with the MLI output voltage THD with normal method, NN method and Fuzzy method. The simulation result reveals that the proposed ANFIS controller out-performs the other previous techniques. It is also seen that the proposed method has smaller THD under various load conditions. A prototype of three-phase grid connected cascaded 5-level inverter has been developed using FPGA. The comparison of experimental result shows that the proposed method is the well-enhanced technique with less harmonics and better efficiency, which is competent over the other techniques.

## References

1. F. Kinninger, Photovoltaic systems technology, Kassel, Germany, Universitat Kassel, Institut fur Rationelle Energiewandlung, 2003.
2. M. Liserre, T. Sauter and J. Y. Hung, Future energy systems: Integrating renewable energy sources into the smart power grid through industrial electronics, *IEEE Industrial Electron. Magaz.* **4** (2010) 18–37.
3. S. Seme, G. Stumberger and J. Voric, Operational properties of a photovoltaic system with three single phase inverters, *International Conference on Renewable Energies and Power Quality* (2010).
4. E. Koutroulis, K. Kalaitzakis and N. C. Voulgaris, Development of a microcontroller-based, photovoltaic maximum power point tracking control system, *IEEE Trans. Power Electron.* **16** (2001) 46–54.

5. I. Houssamo, F. Locment and M. Sechilariu, Maximum power tracking for photovoltaic power system: Development and experimental comparison of two algorithms, *Renewable Energy* **35** (2010) 2381–2387.
6. I. H. Altasa and A. M. Sharaf, A novel maximum power fuzzy logic controller for photovoltaic solar energy systems, *Renewable Energy* **33** (2008) 388–399.
7. S. E. Karatepe and T. Hiyama, Polar coordinated fuzzy controller-based real-time maximum-power point control of photovoltaic system, *Renewable Energy* **34** (2009) 2597–2606.
8. C. Larbes, S. M. A. Cheikh, T. Obeidi and A. Zerguerras, Genetic algorithms optimized fuzzy logic control for the maximum power point tracking in photovoltaic system, *Renewable Energy* **34** (2009) 2093–2100.
9. T. Tafticht, K. Agbossou, M. L. Doumbia and A. Cheriti, An improved maximum power point tracking method for photovoltaic systems, *Renewable Energy* **33** (2008) 1508–1516.
10. A. Chaouachi, R. M. Kamel and K. Nagasaka, A novel multi-model neuro-fuzzy-based MPPT for three-phase grid-connected photovoltaic system, *Solar Energy* **84** (2010) 2219–2229.
11. N. Hamrouni, M. Jraidi and A. Cherif, New control strategy for 2-stage grid-connected photovoltaic power system, *Renewable Energy* **33** (2008) 2212–2221.
12. A. Nabae, I. Takahashi and H. Akagi, A new neutral-point clamped PWM inverter, *IEEE Trans. Industry Appl.* **17** (1981) 518–523.
13. T. A. Maynard and H. Foch, Multi-level choppers for high voltage applications, *Eur. Power Electron. J.* **2** (1992) 45–50.
14. V. Fernaldo Pires, J. F. Martins, D. Foito and Chen Hao, A grid connected photovoltaic system with a multilevel inverter and a Le-Blanc transformer, *Int. J. Renewable Energy Res. Vitor Fernaldo Pires* **2** (2012) 84–91.
15. N. A. Rahim, J. Selvaraj and C. Krismadinata, Five-level inverter with dual reference modulation technique for grid-connected PV system, *Renewable Energy* **35** (2010) 712–720.
16. K. A. Corzine and J. R. Baker, Multilevel voltage-source duty-cycle modulation: Analysis and implementation, *IEEE Trans. Ind. Electron.* **49** (2002) 1009–1016.
17. O. Lopez, A. Alvarez, J. Doval-Gandoy and F. D. Freijedo, Multiphase space vector PWM algorithm, *IEEE Trans. Ind. Electron.* **55** (2008) 1933–1942.
18. J. Chiasson, L. M. Tolbert, K. J. McKenzie and Z. Du, Control of a multilevel converter using resultant theory, *IEEE Trans. Control Syst. Technol.* **11** (2003) 345–354.
19. P. Mattavelli, L. Rossetto, G. Spiazzi and P. Tenti, General-purpose fuzzy controller for dc–dc converters, *IEEE Trans. Power Electron.* **12** (1997) 79–86.
20. S. Saetieo and D. A. Torrey, Fuzzy logic control of a space vector PWM current regulator for three-phase power converters, *IEEE Trans. Power Electron.* **13** (1998) 419–426.
21. C. Cecati, F. Ciancetta and P. Siano, A multilevel inverter for photovoltaic systems with fuzzy logic control, *IEEE Trans. Industrial Electron.* **57** (2010) 4115–4125.
22. R. Seyezhai, B. Kalpana and J. Vasanthi, Design and development of hybrid multilevel inverter employing dual reference modulation technique for fuel cell applications, *Int. J. Power Electronics Drive Syst. (IJPEDS)* **1** (2011) 104–112.
23. R. Chandralekha, G. Shasikala and C. Sasikala, Modeling and analysis of hybrid power systems with power converters, *Int. J. Adv. Eng. Sci. Technol.* **11** (2011) 258–262.
24. C. Vijayalakshmi and R. Latha, Implementation of new single phase multilevel inverter for PV power conditioning system, *Int. J. Adv. Sci. Res. Technol.* **2** (2012) 2249–9954.

25. M. Raghu Vamsi Goutham and M. Venu Gopala Rao, Control of a three-phase cascaded H-bridge multilevel inverter for stand-alone PV system, *Int. J. Modern Eng. Res. (IJMER)* **2** (2012) 278–282.
26. M. V. Rajkumara and P. S. Manoharanb, FPGA based multilevel cascaded inverters with SVPWM algorithm for photovoltaic system, *Solar Energy* **87** (2013) 229–245.
27. Krismadinata, N. Abd Rahim, H. W. Ping and J. Selvaraj, Elimination of harmonics in photovoltaic seven-level inverter with newton-raphson optimization, *Procedia Environmental Sci.* **17** (2013) 519–528.
28. T. R. Sumithira and A. Nirmal Kumar, Elimination of harmonics in multilevel inverters connected to solar photovoltaic systems using ANFIS: An experimental case study, *J. Appl. Res. Technol.* **11** (2013) 124–132.
29. J. J. Mora, G. Carrillo and L. Perez, Fault location in power distribution systems using ANFIS nets and current patterns, *Transmission and Distribution Conference and Exposition Latin America* (2006), pp. 1–6.
30. G. Buticchi, D. Barater, E. Lorenzani, C. Concari and G. Franceschini, A nine-level grid-connected converter topology for single-phase transformerless PV systems, *IEEE Trans. Industrial Electron.* **61** (2014) 3951–3960.
31. J. Mei, B. Xiao, K. Shen, L. M. Tolbert and J. Y. Zheng, Modular multilevel inverter with new modulation method and its application to photovoltaic grid-connected generator, *IEEE Trans. Power Electron.* **28** (2013) 5063–5073.
32. F. Filho, H. Z. Maia, T. H. A. Mateus, B. Ozpineci, L. M. Tolbert and J. O. P. Pinto, Adaptive selective harmonic minimization based on ANNs for cascade multilevel inverters with varying DC sources, *IEEE Trans. Industrial Electron.* **60** (2013) 1955–1962.
33. B. Shanthi and S. P. Natarajan, FPGA based fuzzy logic control for single phase multilevel inverter, *Int. J. Comput. Appl.* **9** (2010) 10–18.